Article

Cell Reports

Fatty Acid Oxidation Mediated by Acyl-CoA Synthetase Long Chain 3 Is Required for Mutant *KRAS* Lung Tumorigenesis

Graphical Abstract

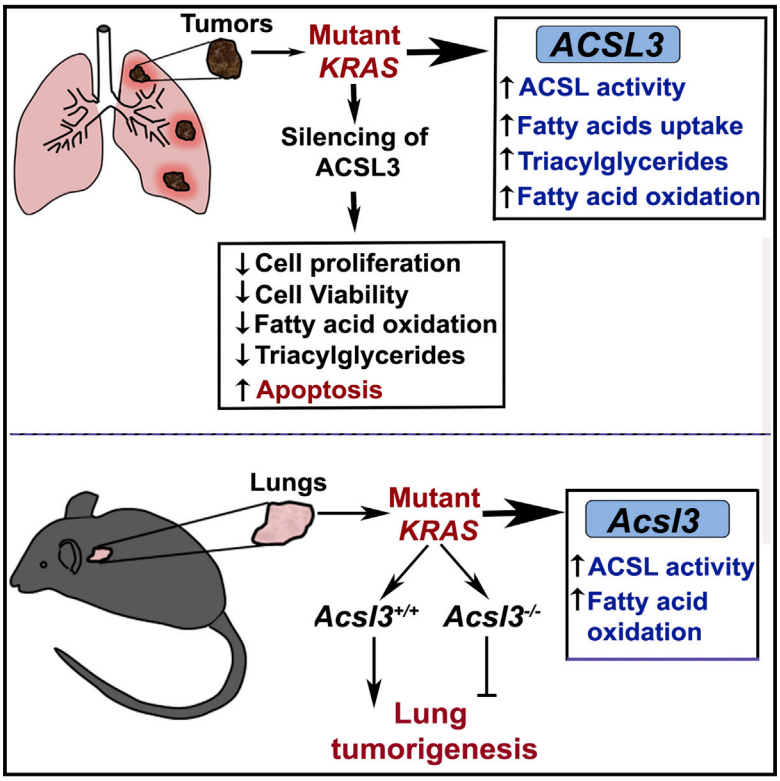

Highlights

- *ACSL3* expression and activity in lung cancer cells is upregulated by mutant *KRAS*
- *ACSL3* suppression decreases β-oxidation and ATP levels in mutant *KRAS* lung cancer cells
- *ACSL3* is required for survival and oncogenic capacity of mutant *KRAS* lung cancer cells
- *ACSL3* is highly expressed in human lung cancer specimens and promotes cancer initiation

Authors

Mahesh S. Padanad, Georgia Konstantinidou, Niranjan Venkateswaran, ..., Ignacio I. Wistuba, Ralph J. DeBerardinis, Pier Paolo Scaglioni

Correspondence

pier.scaglioni@utsouthwestern.edu

In Brief

In Brief: Padanad et al. find that *ACSL3* is the critical enzyme required for viability of mutant *KRAS* lung cancer cells in vitro and for lung cancer initiation and progression in vivo. *ACSL3* mediates survival and tumorigenesis of mutant *KRAS* lung cancer cells by promoting uptake, retention, and β-oxidation of fatty acids.

Accession Numbers

GSE40606

Padanad et al., 2016, Cell Reports *16*, 1614–1628
August 9, 2016
http://dx.doi.org/10.1016/j.celrep.2016.07.009

CellPress

OPEN ACCESS
CellPress

Cell Reports
Article

Fatty Acid Oxidation Mediated by Acyl-CoA Synthetase Long Chain 3 Is Required for Mutant *KRAS* Lung Tumorigenesis

Mahesh S. Padanad,[1,2,12] Georgia Konstantinidou,[1,2,12,13] Niranjan Venkateswaran,[1,2] Margherita Melegari,[2] Smita Rindhe,[1,2] Matthew Mitsche,[3,4] Chendong Yang,[5] Kimberly Batten,[6] Kenneth E. Huffman,[7] Jingwen Liu,[8] Ximing Tang,[9] Jaime Rodriguez-Canales,[9] Neda Kalhor,[9] Jerry W. Shay,[6] John D. Minna,[1,7] Jeffrey McDonald,[4] Ignacio I. Wistuba,[10,11] Ralph J. DeBerardinis,[3,5] and Pier Paolo Scaglioni[1,2,*]

[1]Department of Internal Medicine
[2]Simmons Comprehensive Cancer Center
[3]McDermott Center for Human Growth and Development
[4]Department of Molecular Genetics
[5]Children's Medical Center Research Institute
[6]Department of Cell Biology
[7]Hamon Center for Therapeutic Oncology Research
The University of Texas Southwestern Medical Center, Dallas, TX 75390, USA
[8]Department of Veterans Affairs, Palo Alto Health Care System, Palo Alto, CA 94304, USA
[9]Department of Translational Molecular Pathology
[10]Department of Pathology
[11]Departments of Translational Molecular Pathology and Thoracic/Head and Neck Medical Oncology
MD Anderson Cancer Center, The University of Texas, Houston, TX 7030, USA
[12]Co-first author
[13]Present address: Institute of Pharmacology, Inselspital, INO-F 3010 Bern, Switzerland
*Correspondence: pier.scaglioni@utsouthwestern.edu
http://dx.doi.org/10.1016/j.celrep.2016.07.009

SUMMARY

***KRAS* is one of the most commonly mutated oncogenes in human cancer. Mutant *KRAS* aberrantly regulates metabolic networks. However, the contribution of cellular metabolism to mutant KRAS tumorigenesis is not completely understood. We report that mutant *KRAS* regulates intracellular fatty acid metabolism through *Acyl-coenzyme A* (*CoA*) *synthetase long-chain family member 3* (*ACSL3*), which converts fatty acids into fatty Acyl-CoA esters, the substrates for lipid synthesis and β-oxidation. *ACSL3* suppression is associated with depletion of cellular ATP and causes the death of lung cancer cells. Furthermore, mutant KRAS promotes the cellular uptake, retention, accumulation, and β-oxidation of fatty acids in lung cancer cells in an *ACSL3*-dependent manner. Finally, *ACSL3* is essential for mutant *KRAS* lung cancer tumorigenesis in vivo and is highly expressed in human lung cancer. Our data demonstrate that mutant KRAS reprograms lipid homeostasis, establishing a metabolic requirement that could be exploited for therapeutic gain.**

INTRODUCTION

Lung cancer remains one of the leading causes of cancer-related death. Activating mutations of the proto-oncogene *KRAS* (mutant *KRAS*) occur in ~30% of the cases of non-small cell lung cancer (NSCLC) (Cancer Genome Atlas Research Network, 2014; Pylayeva-Gupta et al., 2011). Continuous expression of mutant *KRAS* is required for the survival of NSCLC both in mouse cancer models and human-derived NSCLC cells (Fisher et al., 2001; Singh et al., 2009). Mutant KRAS promotes tumorigenesis by regulating several oncogenic networks, for instance, the RAF/MEK/ERK, PI3K/AKT/mTOR, and RHOA-focal adhesion kinase. These observations establish mutant KRAS as a therapeutic target. However, there are currently no approved therapies that target tumors that harbor mutant *KRAS* (Gysin et al., 2011; Konstantinidou et al., 2013; Pylayeva-Gupta et al., 2011).

Cancer cells undergo oncogene-directed metabolic reprogramming to support cell growth and survival. For instance, cancer cells harboring mutant *KRAS* display a high level of carbon flux through aerobic glycolysis and activation of glucose-dependent biosynthetic pathways, including the synthesis of hexosamines and nucleotides (Boroughs and DeBerardinis, 2015; Hu et al., 2012; Ying et al., 2012). Therefore, mutant *KRAS* drives both the acquisition of nutrients and the orchestration of cellular metabolism to convert carbon sources into biomass. However, the relevance of metabolic reprogramming in tumorigenesis is not completely understood.

The metabolism of fatty acids (FAs) is emerging as a mechanism to cope with oncogenic stress. For instance, mutant KRAS stimulates the cellular uptake of lysophospholipids, and cancer cells with deregulated mTORC1 are dependent on unsaturated FAs in hypoxic conditions (Kamphorst et al., 2013; Young et al., 2013). Autophagy is also emerging as a mechanism to maintain functional mitochondria, which are important for lipid

metabolism (Guo et al., 2013). However, the mechanistic details of the regulation and the biological significance of the cellular metabolism of FAs in cancer cells are not completely understood.

Fatty acids are fundamental cellular components that may be used as building blocks for cellular membranes, as moieties for post-translational protein modification, and as substrates for energy generation through β-oxidation. De novo FA synthesis involves several key enzymes: ATP citrate lyase (ACL) generates acetyl-coenzyme A (CoA) from citrate, which is typically produced in the mitochondrial tricarboxylic acid cycle (TCA) cycle; acetyl-CoA carboxylase (ACC) catalyzes the irreversible carboxylation of acetyl-CoA to form malonyl-CoA, the committed metabolite in FA synthesis; and fatty acid synthase (FASN) then sequentially adds 2-carbon units until a long-chain FA is produced.

In most tissues, *FASN* expression is low; thus, most non-transformed cells preferentially use dietary (exogenous) lipids for energy generation and membrane maintenance (Menendez and Lupu, 2007). However, proliferating cells avidly take up free FAs from the environment and use them to generate phospholipids, which constitute a substantial fraction of the dry weight of mammalian cells (Deberardinis et al., 2006; Spector, 1967). Furthermore, overexpression of *FASN* occurs in several human cancers, suggesting that some cancer cells and tumors endogenously synthesize FAs (Furuta et al., 2008; Menendez and Lupu, 2007).

Acyl-CoA synthetases (ACSLs) are a family of enzymes (i.e., *ACSL1*, *3*, *4*, *5*, and *6*) that convert free long-chain FAs into fatty acyl-CoA esters, which then serve as a substrate for both lipid synthesis and β-oxidation (Coleman et al., 2002). FAs are not only de novo synthesized but also are taken from exogenous sources. Once FAs are in the cell, ACSLs promote their retention by converting them into hydrophilic fatty acyl-CoA esters that cannot exit cells (Kamp and Hamilton, 2006).

ACSL enzymes utilize a wide range of saturated and unsaturated FAs with a preference for FAs of chain lengths of 8–22; however, they vary greatly in substrate specificity: for instance, *ACSL1* and *ACSL5* prefer oleate, *ACSL3* palmitate, and *ACSL4* arachidonic acid (Grevengoed et al., 2014; Soupene and Kuypers, 2008).

ACSL enzymes are ubiquitously expressed, even though individual genes are differentially expressed in individual tissues and differ in subcellular localization. For instance, ACSL3 is mainly expressed in the endoplasmic reticulum (ER) and lipid droplets and ACSL4 in peroxisomes and ER, whereas ACSL1, ACSL5, and ACSL6 are expressed in mitochondria, plasma membrane, and cytoplasm (Grevengoed et al., 2014; Soupene and Kuypers, 2008). Moreover, ACSL enzymes are expressed in pneumocytes, where they participate in the synthesis of surfactant (Coleman et al., 2002; Schiller and Bensch, 1971).

ACSL enzymes also participate in the metabolic reprogramming of cancer cells. For instance, pharmacologic inhibition of ACSLs results in apoptosis in a subset of TP53-deficient cancer cells (Mashima et al., 2005; Yamashita et al., 2000). Nevertheless, the biological significance of ACSL enzymes in promoting tumorigenesis is still largely unknown. For instance, it remains to be determined whether they play a role in the maintenance of cancers expressing mutant *KRAS*. Furthermore, it is not known whether glucose or fatty-acid-dependent cellular metabolic processes are worthy of therapeutic targeting in *KRAS* tumors.

In this manuscript, we show that *ACSL3* is essential for the oncogenic capacity of mutant *KRAS* in lung cancer. Our data provide the rationale for the development of inhibitors that specifically target ACSL3 as anticancer drugs.

RESULTS

Mutant KRAS Regulates Glycolysis and Lipid Biosynthetic Processes In Vivo

To gain insight into mutant KRAS-regulated cellular networks that are required for tumor maintenance, we employed a transgenic mouse expressing a doxycycline (doxy)-inducible mutant *Kras* transgene in the respiratory epithelium. For this purpose, we crossed tetracycline operator-regulated $Kras^{G12D}$ (*tet-op-*$Kras^{G12D}$) mice with Clara cell secretory protein-tet activator (*CCSP-rtTA*) mice. When fed with doxy, *CCSP-rtTA/tet-op-*$Kras^{G12D}$ mice invariably develop lung tumors, which are dependent on continuous expression of $Kras^{G12D}$ (Fisher et al., 2001).

To obtain well-established lung tumors, we fed *CCSP-rtTA/tet-op-*$Kras^{G12D}$ mice with doxy for 11 weeks. In agreement with previous findings, withdrawal of doxy from the diet caused $Kras^{G12D}$ extinction (Figure 1A; Fisher et al., 2001). Accordingly, total RAS activity and activated PDK1, a well-known downstream target of KRAS, were also downregulated (Figures 1B and 1C). Lung tumors completely regressed 6 days after doxy withdrawal (Figure 1D).

To identify proximal molecular changes linked to $Kras^{G12D}$ extinction, we performed whole-genome gene expression analysis of micro-dissected lung tumors 24 or 48 hr after doxy withdrawal. Database for Annotation, Visualization and Integrated Discovery-based (DAVID) functional enrichment analysis and gene set enrichment analysis (GSEA) between experimental groups revealed a significant downregulation of genes that regulate glycolysis and lipid metabolic processes in mice undergoing $Kras^{G12D}$ withdrawal (Figures 1E–1G; data not shown).

Mutant $Kras^{G12D}$ extinction significantly downregulates the expression of the glycolytic enzymes *hexokinase 2* (*Hk2*) and *lactate dehydrogenase-A* (*Ldh-A*) in lung tumors in vivo (Figure 1H). This observation is consistent with the fact that mutant KRAS has been associated with increased lactate production in cancer cells in vitro (Yun et al., 2009). Furthermore, *Hk2* and *Ldh-A* play an important role in mutant *Kras*-driven lung tumorigenesis (Patra et al., 2013; Xie et al., 2014). However, we found that silencing of glycolytic enzymes decreases cell proliferation, glucose consumption, and lactate production without causing overall cell loss in vitro (Figures S1A–S1F).

Mutant KRAS Upregulates *ACSL3* and *ACSL4*

We found that the lipid metabolic enzymes *Acsl3* and *Acsl4* were significantly downregulated in mouse lung tumors undergoing $Kras^{G12D}$ extinction, whereas we did not detect significant changes in mRNA levels of their family members *Acsl1*, *Acsl5*, and *Acsl6* (Figure 1I). Furthermore, $Kras^{G12D}$ lung tumors display

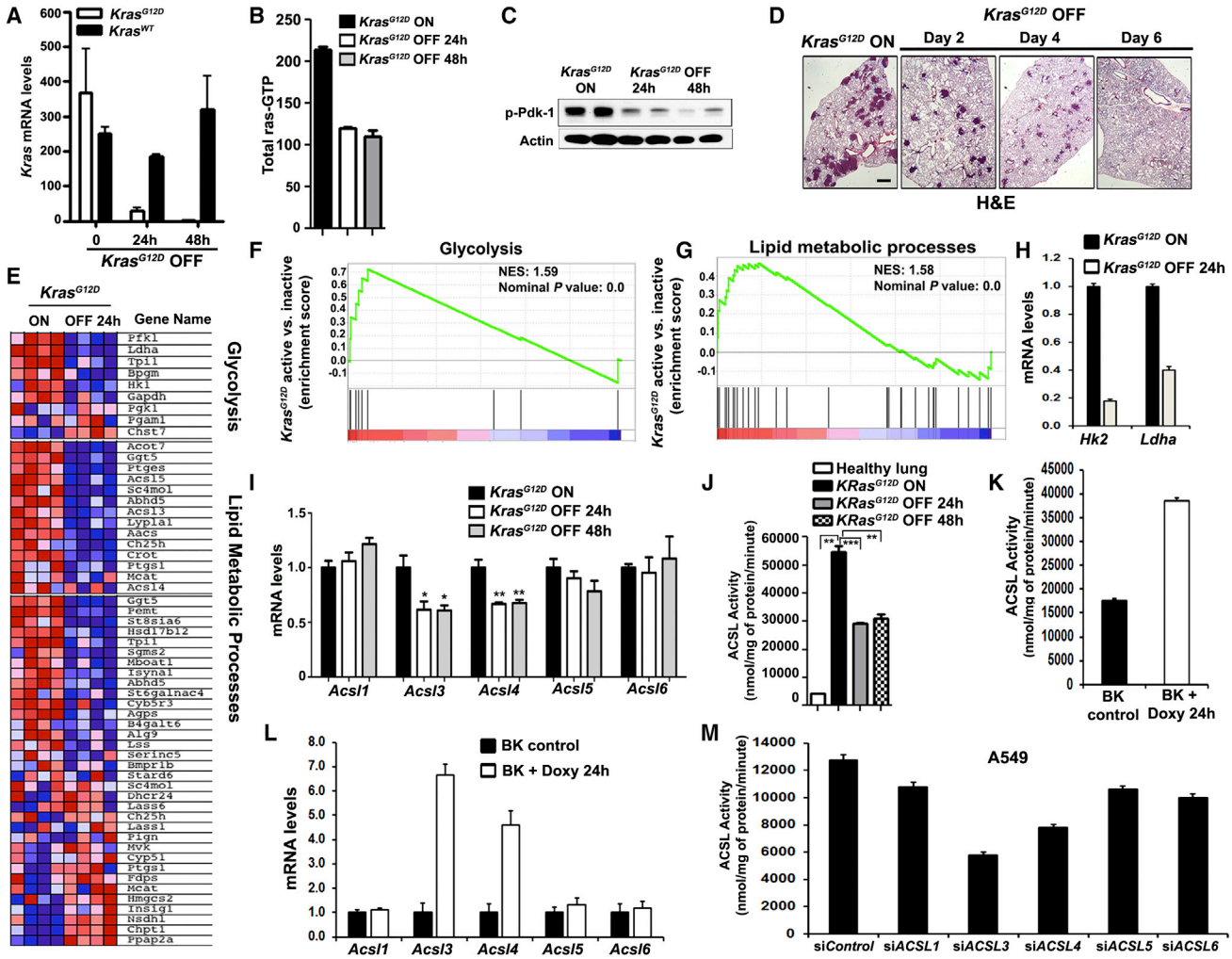

Figure 1. Mutant *KRAS* Regulates *ACSL3* and *ACSL4* in Lung Cancer Cells Both In Vitro and In Vivo

(A) Transgenic ($Kras^{G12D}$) and endogenous ($Kras^{WT}$) mRNA was quantified in micro-dissected lung tumors of *CC10-rtTA/Tet-op-*$Kras^{G12D}$ mice by real-time PCR at the indicated time points after doxy withdrawal.

(B) Pan-Ras activity was measured with an ELISA assay in micro-dissected lung tumors at the indicated time points after doxy withdrawal in *CC10-rtTA/Tet-o-*$Kras^{G12D}$ mice; ***$p < 0.0003$.

(C) Immunoblot detection of P-Pdk1 in lysates of micro-dissected lung tumors at the indicated time points after $Kras^{G12D}$ extinction.

(D) H&E-stained lung tissue sections demonstrating lung tumor regression at the indicated time points after $Kras^{G12D}$ extinction; the scale bar represents 1 mm.

(E) Heatmaps of the genes found enriched in a genome-wide expression profiling, illustrating the changes in gene expression of the indicated metabolic pathways 24 hr upon doxy withdrawal. Expression level shown is representative of $\log_2$ values of each replicate from micro-dissected lung tumors (n = 4). Red signal denotes higher expression relative to the mean expression level within the group, and blue signal denotes lower expression relative to the mean expression level within the group.

(F) GSEA plot of glycolytic processes based on the 24-hr off-doxy versus on-doxy gene expression profiles. NES, normalized enrichment score; p, nominal value.

(G) GSEA plot of and lipid metabolic processes based on the 24-hr off-doxy versus on-doxy gene expression profiles.

(H) Real-time PCR showing mRNA levels of *Hk2* and *Ldh-A* in lung tumors of $Kras^{G12D}$ mice before or 24 hr after $Kras^{G12D}$ extinction.

(I) Real-time PCR showing mRNA levels of *Acsl* family members in lung tumors of $Kras^{G12D}$ mice before or 24–48 hr after $Kras^{G12D}$ extinction. *$p < 0.02$; **$p < 0.004$.

(J) ACSL enzymatic activity in healthy lung parenchyma or in micro-dissected lung tumors after 11 weeks of $Kras^{G12D}$ induction or after the indicated length of $Kras^{G12D}$ extinction. **$p < 0.003$; ***$p < 0.001$.

(K) ACSL enzymatic activity measured in BK fibroblasts treated with doxy for 24 hr.

(L) Real-time PCR showing mRNA levels of *Acsl* family members in BK fibroblasts treated with doxy for 24 hr.

(M) ACSL enzymatic activity in A549 NSCLC cells after transfection with the indicated siRNAs.

See also Figure S1.

a striking upregulation of ACSL enzymatic activity compared to lung tissue of non-transgenic littermates (Figure 1J). Conversely, ACSL activity is downregulated by about 50% in lung tumors as early as 24 hr after $Kras^{G12D}$ extinction (Figure 1J). These findings suggest that ACSL enzymatic activity plays a significant role in the maintenance of mutant *KRAS* lung cancer.

We tested whether *Acsl3* and *Acsl4* are dependent on $Kras^{G12D}$ in cell culture with several complementary approaches. We found that $Kras^{G12D}$ induction increases ACSL activity and selectively upregulates *Acsl3* and *Acsl4* mRNA levels (Figures 1K, 1L, and S1G) in mouse embryonic fibroblasts derived from tetracycline operator-regulated Tet-op-$Kras^{G12D}$;$p53^{-/-}$ transgenic mice (hereafter BK cells). These cells stably express *rtTA*, allowing tight doxy-dependent expression of $Kras^{G12D}$ (Pao et al., 2003).

Next, to demonstrate that $Kras^{G12D}$ upregulates *Acsl3*, we performed transactivation assays in BK cells. We observed that $Kras^{G12D}$ increases approximately by 3-fold the activity of an *ACSL3* promoter reporter (pGL3-*ACSL3luc*; Figure S1H; Cao et al., 2010). Furthermore, treatment with rapamycin, a well-known inhibitor of mTORC1, inhibits the ability of KRAS to upregulate the *ACSL3* promoter reporter (pGL3-*ACSL3luc*; Figure S1I) and also *Acsl3* mRNA (Figure S1J). These findings suggest that mutant KRAS regulates ACSL3 expression through the mTOR signaling pathway. In addition, *KRAS* silencing reduces ACSL activity by about 50% in several NSCLC cells (Figure S1K and S1L). Finally, silencing of *KRAS* with a siRNA pool significantly reduced *ACSL3* mRNA levels (Figure S1M).

We silenced each of the ACSL family members (i.e., *ACSL1*, *ACSL3*, *ACSL4*, *ACSL5*, and *ACSL6*) to determine their relative contribution to ACSL cellular activity in mutant KRAS NSCLC cells: knockdown of *ACSL3* leads to the largest reduction of total ACSL activity followed by the knockdown of *ACSL4*. However, knockdown of *ACSL1*, *ACSL5*, and *ACSL6* had modest to no effect on total ACSL activity (Figures 1M and S1N).

Taken together, these results indicate that mutant KRAS regulates ACSL activity both in vivo and in vitro and that ACSL3 is the functionally predominant ACSL gene in mutant *KRAS* NSCLC.

ACSL3 Is Required for the Survival of Mutant KRAS In Vitro

In order to investigate whether ACSL3 promotes the survival of lung cancer cells expressing mutant *KRAS*, we silenced *ACSL3* in a panel of human NSCLC cells, which have been extensively characterized with respect to the presence of oncogenic mutations (Sanger Institute Catalogue of Somatic Mutations in Cancer and the Cancer Genome Atlas; Table S1). *ACSL3* silencing with two non-overlapping short hairpin RNAs (shRNAs) striking reduced the proliferation of ten mutant *KRAS* NSCLC cell lines and less-pronounced but still statistically significant inhibitory effects in the mutant *KRAS* HCC4017 and HCC461 cells (Figures 2A, 2B, and S2A). These NSCLC cell lines, with the exception of HCC461, carry also mutations inactivating the *TP53* and/or *INK4A/ARF* tumor suppressors. Notably, *ACSL3* silencing did not cause significant antiproliferative effects in immortalized human bronchial epithelial cells (HBEC3KT cells) that ectopically express mutant *KRAS* (Ramirez et al., 2004). In contrast, the effect of *ACSL3* silencing on cell viability was not consistent in lung cancer cells carrying wild-type KRAS: we did not detect significant adverse effects in six lung cancer cells (H522, H596, H838, H1437, H2023, and HCC15) that harbor wild-type *KRAS* but are mutant for either *TP53* or *INK4A/ARF* (Figures 2A and 2B). However, *ACSL3* knockdown leads to inhibitory effects in H125 (wild-type *KRAS*; *TP53*;*INK4A/ARF* mutant), H661 (wild-type *KRAS*; *TP53*;*INK4A/ARF* mutant), and HCC95 (wild-type *KRAS*; *TP53* mutant) lung cancer lines (Figure S2B). In addition, there was no correlation between dependency on ACSL3 and the proliferation rates of these NSCLC cells (Figure 2A; Table S1). Among the cell lines that were used for cell proliferation assays, with exception for H1264, there was a positive correlation between ACSL3 abundance and sensitivity to *ACSL3* knockdown (Figures 2B and S2C).

To assess off-target effects, we performed rescue experiments with retroviruses expressing *ACSL3* cDNAs harboring mutations ablating binding sites of either shRNA *ACSL3* (A) or shRNA *ACSL3* (B), named *ACSL3* mutant 1 and *ACSL3* mutant 2, respectively (Figure 2C). The antiproliferative effect caused by shRNA *ACSL3* (A) was rescued by *ACSL3* mutant 1, but not by mutant 2 (Figure 2D). Conversely, the phenotype of shRNA *ASCL3* (B) was rescued by *ACSL3* mutant 2, but not by mutant 1 (Figure 2D). As expected, cells expressing the shRNA-resistant *ACSL3* cDNAs had increased levels of ACSL3 as compared to cells expressing wild-type *ACSL3* cDNA (Figure S2D). Thus, we conclude that the antiproliferative effects are specific to *ACSL3* knockdown and not due to off-target effects.

Next, we tested the effect of knocking down *ACSL4*, which is also downregulated by mutant *Kras* extinction in lung tumors (Figure 1I). However, knocking down *ACSL4* both in mutant and wild-type *KRAS* cells did not cause any significant effect on cell proliferation (Figure S2E).

To begin assessing the mechanism underlying the dependency on *ACLS3*, we assessed the effect of its silencing on ACSL activity. We found that knockdown of *ACSL3* reduced ACSL activity by 55%–65% in mutant *KRAS* NSCLC cells but only by 30%–35% in wild-type *KRAS* cells (Figure S2F). In addition, *ACSL3* knockdown leads to the cell-line-dependent upregulation of *ACSL1*, *ACSL4*, and *ACSL6* in wild-type *KRAS* lung cancer cells that are resistant to *ACSL3* knockdown (Figures S2G and S2H). In contrast, knockdown of *ACSL4* reduced ACSL activity only by 20%–30% in representative mutant *KRAS* and wild-type *KRAS* NSCLC cells (Figures S2I and S2J). Finally, we found that ACSL3 knockdown did not affect glucose or glutamine consumption neither in mutant nor in wild-type *KRAS* lung cancer cells (Figures S2K and S2L; data not shown). Taken together, these results indicate that (1) mutant KRAS regulates ACSL activity both in vivo and in vitro, (2) ACSL3 is the functionally predominant ACSL isoenzyme in mutant *KRAS* lung cancer cells, (3) upregulation of other *ACSL* family members and not glycolysis or glutaminolysis is likely to mediate the resistance to *ACSL3* knockdown in wild-type *KRAS* lung cancer cells, and (4) the decrease of ACSL activity caused by *ACSL4* knockdown is below the threshold needed to cause detrimental effects on cell viability.

Characterization of the Role of ACSL3 in Mutant KRAS Lung Cancer Cells

ACSL3 silencing was accompanied by induction of apoptosis, as shown by an increase in the percentage of the $SubG_0$ population of cells, cleaved poly (ADP-ribose) polymerase (PARP) and cleaved caspase 3 in H460, H1264, and HCC44 cells, as representative examples of ACSL3-dependent lung cancer cells

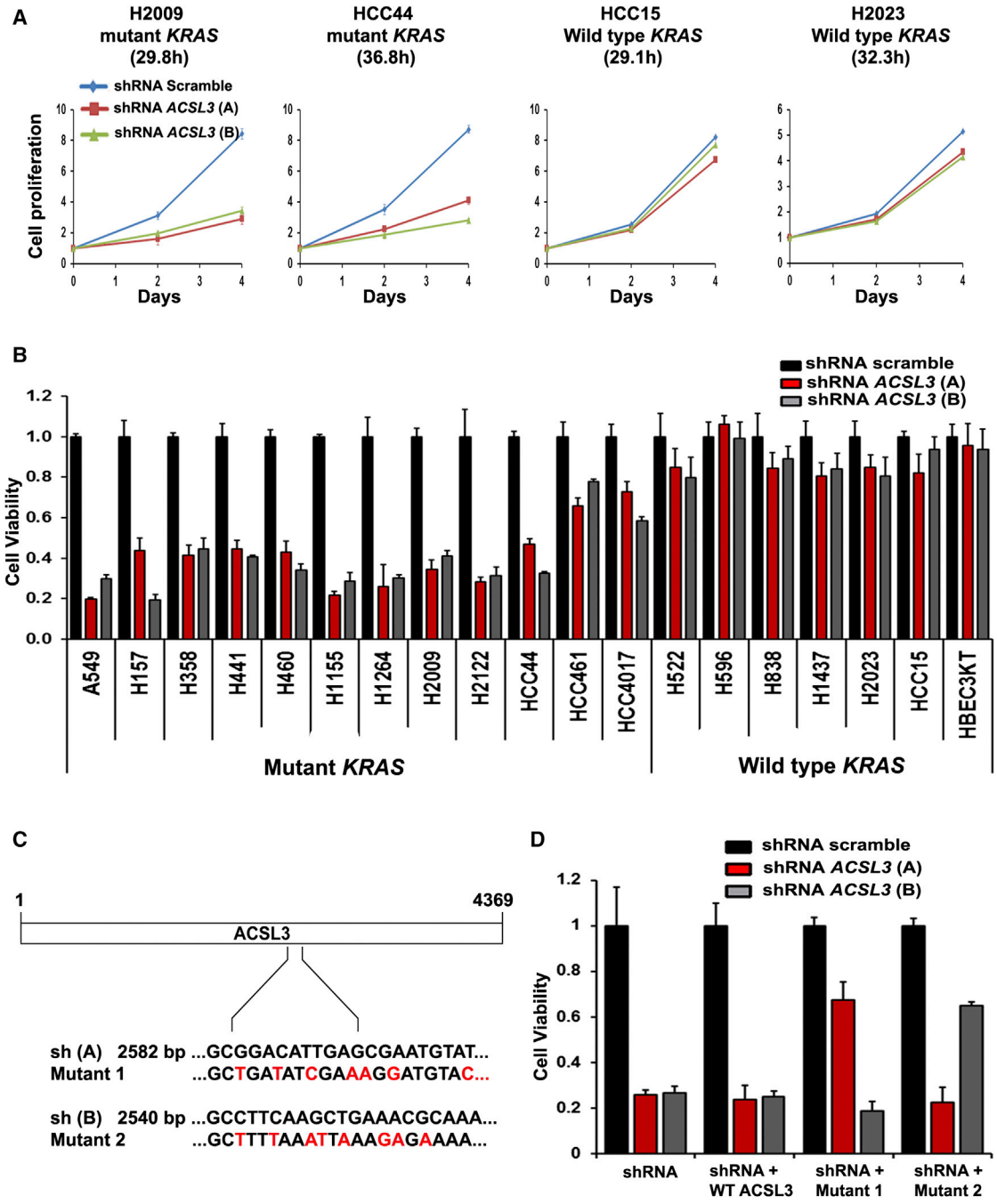

Figure 2. *ACSL3* Is Required for the Proliferation of NSCLC Cells Expressing Mutant *KRAS*

(A) Growth curves of NSCLC cells upon transduction with the indicated shRNAs. *KRAS* status for each cell line is indicated. Doubling time is mentioned in hours in parentheses.

(B) The histogram shows cell viability of the indicated NSCLC cells 96 hr after transfection with *ACSL3* or control shRNAs.

(C) Schematic representation of the *ACSL3* rescue cDNA mutants. shRNA recognition site and sequence of shRNA mutant 1 and 2 are indicated. Red letters indicate mutated nucleotides.

(D) The histogram shows H460 (mutant *KRAS*) cell viability of lung cancer cell line transduced with retroviruses expressing the indicated shRNA and *ACSL3* cDNAs.

See also Figure S2 and Table S1.

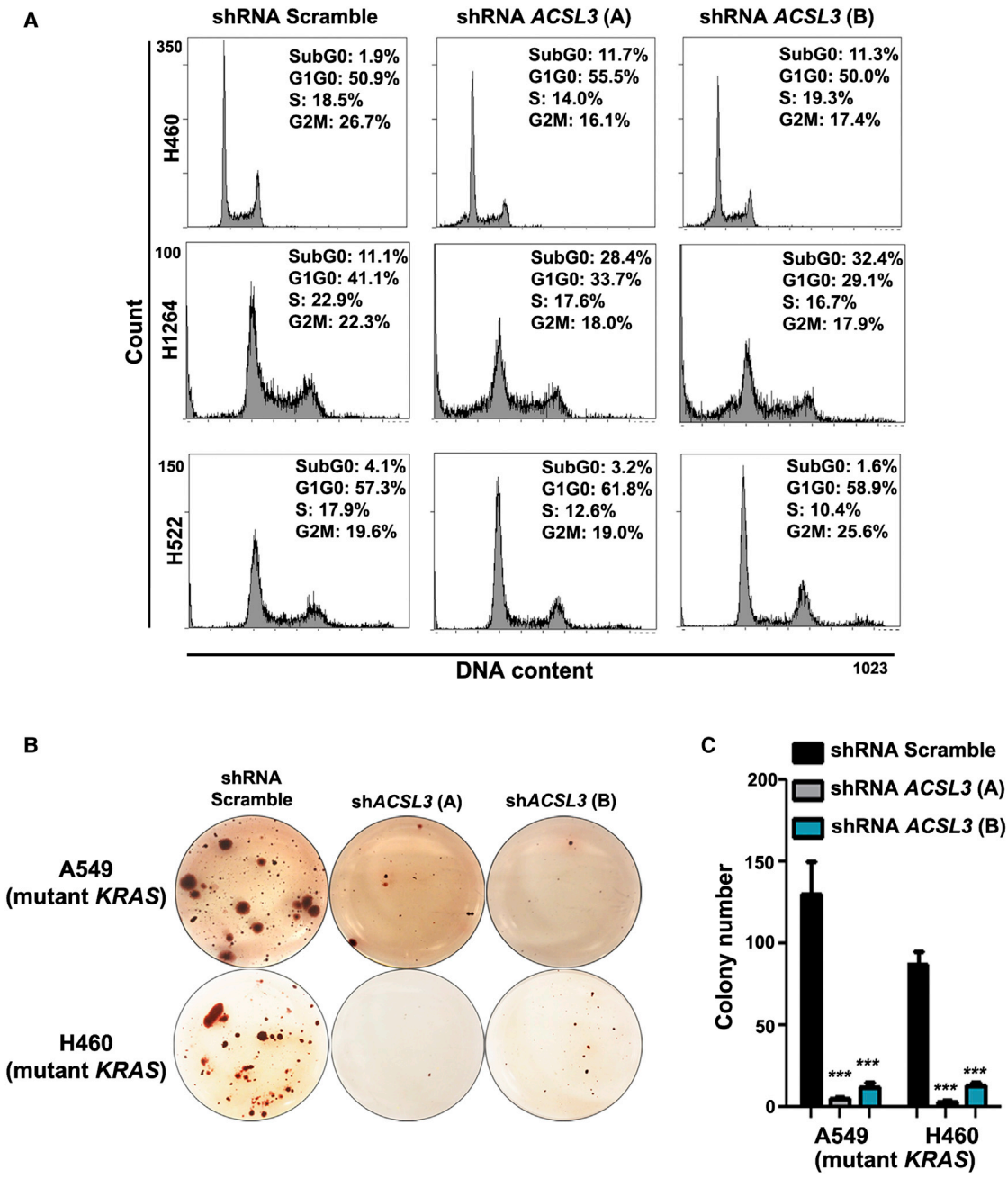

Figure 3. *ACSL3* Is Required for the Survival and Anchorage-Independent Growth of NSCLC Cells Expressing Mutant *KRAS*

(A) Flow cytometry showing the effect of shRNA-mediated *ACSL3* knockdown on cell cycle of the indicated NSCLC lines. The percentages of cells in specific phases of the cell cycle are indicated. Note the presence of cells in the sub-G0 phase of the cell cycle in the *ACSL3*-dependent H460 and H1264 cells, but not in the *ACSL3*-independent H522 cells.

(B) Representative images of tissue culture plates showing soft agar colony formation assay in A549 and H460 (mutant *KRAS*) cells treated as indicated.

(C) Histograms showing quantification of colonies of A549 and H460 cells grown in soft agar upon transduction with the indicated shRNAs; ***$p < 0.001$.

See also Figure S3.

(Figures 3A, S3A, and S3B). These changes were not evident in H522 NSCLC cells, which are representative of the cells refractory to *ACSL3* silencing (Figure 3A). In addition, we measured mitochondrial membrane potential using JC-1 (5, 5′, 6, 6’-tetracholoro-1, 1’, 3, 3′-tetraethylbenzimi-dazolylcarbocyanine iodide), a cytofluorimetric lipophilic cationic dye. Silencing of *ACSL3* leads to significant decrease in membrane potential in H460 mutant *KRAS* cells (Figure S3C), which is consistent with induction of apoptosis. Next, we assessed the effect of silencing *ACSL3* on mitochondrial respiratory activity. We found that

ACSL3 silencing significantly reduces basal oxygen consumption rate (OCR) in real time in H460 mutant *KRAS* cells (Figure S3D). These results lend further support to the notion that lung cancer cells that express mutant *KRAS* are vulnerable to *ACSL3* depletion.

To interrogate the functional significance of *ACSL3* in KRAS lung tumorigenesis, we performed colony formation assays in soft agar and found that shRNA-mediated *ACSL3* silencing results in more than 90% inhibition of colony formation in A549, H460, and H1155, mutant *KRAS* NSCLC cells, but caused no significant inhibition of colony formation in HCC15 and H2023 wild-type KRAS NSCLC cells (Figures 3B, 3C, S3E, and S3F). These results indicate that *ACSL3* is critical for maintaining the ability of mutant *KRAS* NSCLC cells to grow in an anchorage-independent fashion, which is a hallmark of cancer cells (Hanahan and Weinberg, 2011).

Taken together, these results support several conclusions: (1) *ACSL3* plays a critical role in promoting the survival of mutant *KRAS* NSCLC cells; (2) silencing of *ACSL*3 does not lead to generalized antiproliferative or proapoptotic effects, as demonstrated by its inability to impair H522, H596, H838, H1437, H2023, HCC15, and HBEC3KT cells; and (3) *ACSL3* may exert a prosurvival function in NSCLC cells carrying oncogenotypes other than mutant *KRAS*, as demonstrated by the inhibitory effects we observed upon *ACSL3* knockdown in H125, H661, and HCC95 cells.

ACSL3 Promotes Fatty Acid Uptake, Accumulation of Neutral Lipids, and β-Oxidation in Mutant *KRAS* NSCLC Cells

Although mutant *KRAS* cancer cells display both de novo FA synthesis and lipid uptake from extracellular sources, it is not known which pathways predominate. It is also unknown whether mutant KRAS cells predominantly utilize these FAs as a substrate for the synthesis of structural or storage lipids, for instance, phospholipids or triacylglycerides (TAGs), and/or for energy production by β-oxidation (Boroughs and DeBerardinis, 2015).

We observed that $Kras^{G12D}$ extinction in vivo leads to a time-dependent (24–48 hr) downregulation of a set of genes known to control FA entry into the mitochondria/peroxisomes or ER. In particular, we detected genes responsible for long-chain FA transport and FA oxidation (Figures 4A–4C, S4A, and S4B). These observations suggest that KRAS enhances the expression of genes involved in β-oxidation.

In order to gain insight into the impact of mutant KRAS on FA uptake, synthesis of storage/structural lipids, and β-oxidation, we employed isogenic BK cells. We found that mutant KRAS increases the uptake of FAs from an exogenous source in BK cells pulse labeled with the fluorescent FA BODIPY 500/510 C4,9, which mimics a long-chain FA (BODIPY-FA) (Figures 4D and 4E; Kasurinen, 1992; Nchoutmboube et al., 2013). Conversely, *ACSL3* silencing significantly decreases the uptake and cellular retention of fluorescent BODIPY-FA in NSCLC cells (Figures 4F, 4G, and S4C).

To better understand the role of mutant KRAS in cellular lipid metabolism, we used a mass spectrometry method to measure a lipidomic profile, including hundreds of TAGs, 250 phospholipids, cholesteryl esters, diacylglycerides, and free FAs (Fahy et al., 2009; Mitsche et al., 2015). We found that induction of mutant *KRAS* for 24 hr in BK cells increased TAGs and caused an equivalent downregulation of lysophosphatidylcholine (LPC) (Figures 4H and S4D; Table 1). This finding is consistent with the observation that BODIPY-FA accumulates in structures that resemble lipid droplets, the storage site for neutral lipids (Figures 4D–4F and S4C).

Direct quantification of lipid classes indicates that the increase in neutral lipids is accounted by an increase in diacylglycerides (DAGs) and TAGs lipid species, which is consistent with the hypothesis that LPCs are consumed in the synthesis of DAGs and TAGs (Figures 4H and S4E). Conversely, *ACSL3* knockdown decreases the intracellular content of TAGs (Figures 4I, S4E, and S4F; Table 2). Figures S4G and S4H show a summary of the composition of TAGs, phosphatidylcholines, and lysophosphatidylcholines with respect to their number of carbons and double bonds in BK cells and in H460 prior and after doxy treatment or *ACSL3* knockdown, respectively.

In addition, knockdown of *ACSL3* inhibits β-oxidation to a degree similar to etomoxir, a known inhibitor of carnitine palmitoyltransferase, the rate-limiting enzyme that allows entry of acyl-CoA FAs into the mitochondrion (Figure 4J; Pike et al., 2011). Notably, knockdown of *ACSL3* inhibits ATP production to a degree similar to that of cells treated with etomoxir (Figure 4K). Importantly, etomoxir impairs cell viability in this context (Figure 4L). Similarly, 4-bromocrotonic acid, an inhibitor of mitochondrial thiolase, a component of β-oxidation, reduces the cell viability (Figure 4M).

These findings support the conclusion that *ACSL3* in mutant *KRAS* NSCLC critically regulates the uptake and cellular retention of long-chain fatty acyl-CoAs and their channeling to β-oxidation for energy generation. Taken together, these data suggest that inhibition of ACSL3 in vivo would have potent antitumor effects.

ACSL3 Suppression Impairs Tumor Growth In Vivo

To gain insight into the significance of *ACSL3* inhibition in vivo, we performed xenograft experiments using A549 and H460 NSCLC cells, which are representative of our in vitro studies. Silencing *ACSL3* with shRNA(A), which we previously validated to be specific, resulted in a remarkable suppression of tumor formation with 3.5-fold and 10-fold difference compared to the control A549 and H460 xenografts, respectively (Figures 5A and 5B). Significantly, mice carrying xenografts with silenced *ACSL3* had also a dramatically increased survival (Figures 5C and 5D). These results indicate that ACSL3 is required for the tumor growth in vivo.

Loss of *Acsl3* Results in Defective Tumorigenesis in Mutant *Kras* Lung Cancer in Mice

We obtained mutant mice carrying a gene trap disrupting *Acsl3* upstream of exon 1. $Acsl3^{-/-}$ mice were characterized as null based on the absence of transcripts by real-time PCR (LEXKO 011 mouse strain; European Mutant Mouse Archive; Figure S5A). We confirmed the genotype of these mice with a genotyping protocol that distinguishes between wild-type, heterozygous, and homozygous littermates (Figure S5B).

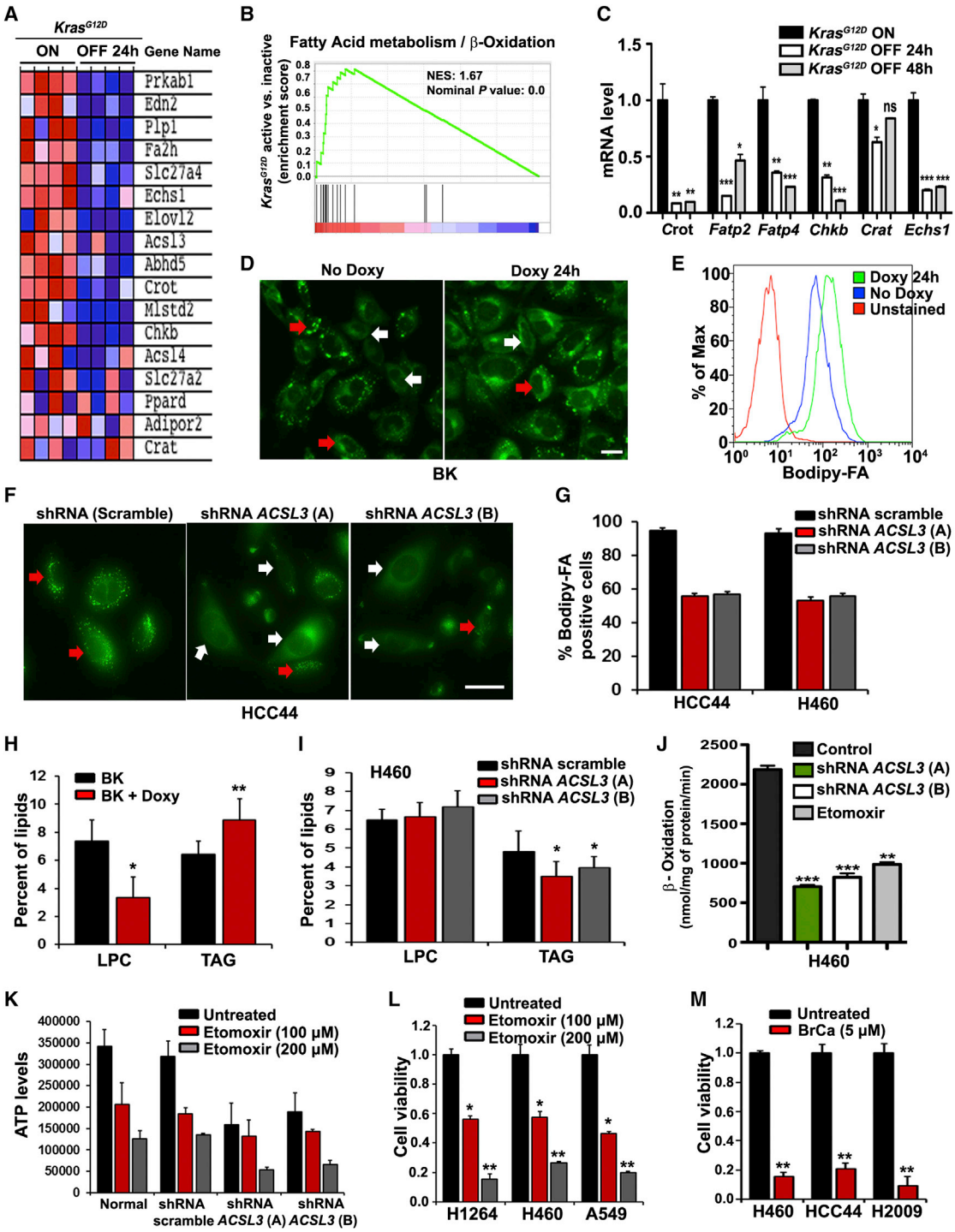

Figure 4. Suppression of Fatty Acids Uptake and β-Oxidation upon Mutant *KRAS* Suppression

(A) Heatmaps illustrating the changes in expression of FA metabolism/β-oxidation genes 24 hr upon doxy withdrawal in mutant *Kras* lung cancer tumors in transgenic mice. Expression level shown is representative of $\log_2$ values of each replicate from micro-dissected lung tumors. Red signal, higher expression; blue signal, lower expression relative to the mean expression level within the group.

(B) GSEA plot of FA metabolism/β-oxidation genes based on the 24-hr off-doxy versus on-doxy gene expression profiles.

(C) Real-time PCR showing the mRNA level of the indicated genes upon $Kras^{G12D}$ extinction in vivo; genes responsible for long-chain FA transport *carnitine O-octanoyltransferase* (*Crot*) and *fatty acid transporter-member 2* (*Fatp2*/*Slc27a2*) and *4* (*Fatp4*/*Slc27a4*); and genes that control FA β-oxidation, such as *enoyl coenzyme A hydratase* (*Echs1*) and *carnitine O-acetyltransferase* (*Crat*); ns, statistically non-significant; *p < 0.01; **p < 0.003; ***p < 0.001.

(legend continued on next page)

Table 1. Cellular Lipids Composition in BK Cells with KRAS Induction

Lipid Classes	BK Cells (%)	BK Cells + Dox (%)
Endocyne	0.02 ± 0.0	0.02 ± 0.0
Lysophospholipids	7.48 ± 1.6	3.44 ± 1.5*
Neutral lipids	8.43 ± 1.1	11.38 ± 1.9**
Phospholipids	76.86 ± 6.3	78.24 ± 2.1
Polar lipids	7.20 ± 1.32	6.92 ± 1.5

Data shown are the mean ± SD of percentage of total lipids at a steady state. Mutant KRAS was induced in BK cells by doxycycline (Dox) treatment for 24 hr. *p < 0.05; **p < 0.001.

Table 2. Cellular Lipids Composition in H460 NSCLC Cells with shRNA against *ACSL3*

Lipid Classes	Scrambled shRNA (%)	shRNA *ACSL3*(A) (%)	shRNA *ACSL3*(B) (%)
Endocyne	0.02 ± 0.0	0.02 ± 0.0	0.02 ± 0.0
Lysophospholipids	6.76 ± 1.6	6.95 ± 0.8	7.46 ± 0.9
Neutral lipids	7.45 ± 1.1	5.58 ± 0.9*	6.00 ± 0.5*
Phospholipids	78.81 ± 6.3	81.08 ± 0.5	79.82 ± 0.9
Polar lipids	6.96 ± 1.3	6.36 ± 0.5	6.69 ± 0.5

Data shown are the mean ± SD of percentage of total lipids at a steady state. *p < 0.05.

We found that *Acsl3*$^{-/-}$ mice are born according to the expected Mendelian ratio, without obvious macroscopic defects during development or adult life. Histologically, lung tissue has no morphological differences between the wild-type and *Acsl3*$^{-/-}$ littermates (Figure S5C). Considering that type II pneumocytes and Clara cells are the probable precursor for lung tumors (Sutherland et al., 2014; Xu et al., 2012), it is noteworthy that there are no significant morphological differences between wild-type and *Acsl3*$^{-/-}$ littermates as confirmed with SP-C (surfactant-associated protein-C) and CCSP staining (Figure S5D). Furthermore, RAS is present at comparable levels in the lungs of wild-type and mutant littermates (Figure S5E). Nevertheless, the lungs of *Acsl3*$^{-/-}$ mice show about 40% decrease in ACSL enzymatic activity as compared to their wild-type littermates (Figure S5F). We conclude that, even though the loss of *Acsl3* significantly decreases the ACSL activity in the lungs, the overall morphology of the lungs is not affected.

To assess the role of *Acsl3* in mutant *Kras* lung tumors in vivo, we generated compound mutant mice by crossing *LSL-Kras*^{G12D} mice (*LSL-Kras* mice) with *Acsl3* mutant mice, which allows conditional expression of *Kras*^{G12D} upon exposure to Cre recombinase in the respiratory epithelium (Jackson et al., 2001). We assessed lung tumorigenesis 8 weeks after intratracheal delivery of an adenovirus that expresses Cre recombinase (adeno-Cre). As expected, ACSL3 is undetectable in the lungs of *Ascl3*$^{-/-}$ mice and a pan-RAS antibody did not detect differences between *Kras*^{G12D};*Acsl3* wild-type and *Kras*^{G12D};*Acsl3*$^{-/-}$ mice (Figure S5G). We assessed tumor number and grade according to well-established diagnostic criteria developed for *Kras*-driven lung cancer mouse models (DuPage et al., 2009; Jackson et al., 2001). The overall tumor burden was significantly decreased in *LSL-Kras*^{G12D};*Acsl3*$^{-/-}$ mice as compared to their *LSL-Kras*^{G12D};*Acsl3*$^{+/+}$ littermates. As expected, in *LSL-Kras*^{G12D};*Acsl3*$^{+/+}$ mice, we detected adenomas with uniform nuclei (A), atypical adenomatous hyperplasia (AAH), and bronchial hyperplasia (BH) (Figures 6A and 6B). In contrast, there were no adenomas in the *LSL-Kras*^{G12D};*Acsl3*$^{-/-}$ mice and all lesions present were small areas of AAH or BH (Figures 6A and 6B). We confirmed that the adenomas and AAH originated from type II alveolar cells with SP-C staining (Figure 6C). In both genotypes, there was equivalent activation of phospho-S6 (P-S6), which is one of the downstream targets of KRAS (Figure 6D). However, AAH lesions of *Kras*^{G12D};*Acsl3*$^{-/-}$ mice had decreased phospho-histone 3 (p-H3) as compared to the ones of *LSL-Kras*^{G12D};*Acsl3*$^{+/+}$ mice (Figures 6D and 6E). These findings suggest that, even though *Acsl3* loss does not affect mutant KRAS signaling, it significantly impairs the capacity of *Kras*^{G12D} to promote cell proliferation and tumor initiation in vivo.

ACSL3 in Human NSCLC

To determine whether *ACSL3* has any significance in patients, we assessed ACSL3 by immunohistochemistry (IHC) on a tissue microarray (TMA) comprising 182 NSCLC patient samples. We found low-level ACSL3 staining in type II pneumocytes of normal lungs, whereas it is readily detectable in NSCLC specimens

(D) BODIPY-FA uptake in BK cells treated with doxy as indicated. Red and white arrows indicate positive and negative cells, respectively (cells with both cytoplasmic and membrane staining were considered positive); the scale bar represents 50 μm. Note that mutant *KRAS* induces the uptake/retention of BODIPY-FA.

(E) Fluorescence-activated cell sorting analysis of BK cells after a 30-min pulse labeling with BODIPY-FA. Note uptake/retention of BODIPY-FA in BK cells expressing mutant *KRAS*.

(F) BODIPY-FA retention in mutant *KRAS* HCC44 NSCLC cells expressing the indicated shRNAs. Red and white arrows indicate representative positive and negative cells, respectively; the scale bar represents 50 μm.

(G) The histogram shows the percentage of BODIPY-FA-positive HCC44 and H460 cells transduced with indicated *ACSL3* shRNA (100 cells were counted in three separate areas).

(H) Composition of lysophosphatidylcholine (LPC) and triacylglycerides (TAGs) in BK cells with and without doxy treatment (*p < 0.05; **p < 0.001).

(I) Composition of LPC and TAGs in H460 NSCLC cells treated with the indicated *ACSL3* shRNA (*p < 0.05).

(J) β-oxidation assay in H460 NSCLC cells treated with the indicated *ACSL3* shRNAs or etomoxir; ***p < 0.001.

(K) Measurement of ATP in H460 NSCLC cells treated with the indicated *ACSL3* shRNAs or etomoxir.

(L) The histogram shows the viability of the indicated mutant *KRAS* NSCLC cells 72 hr after the indicated treatments; *p < 0.01; **p < 0.004.

(M) The histogram shows the viability of the indicated mutant *KRAS* NSCLC cells 72 hr after the treatment with 4-bromocrotonic acid; **p < 0.004.

See also Figure S4.

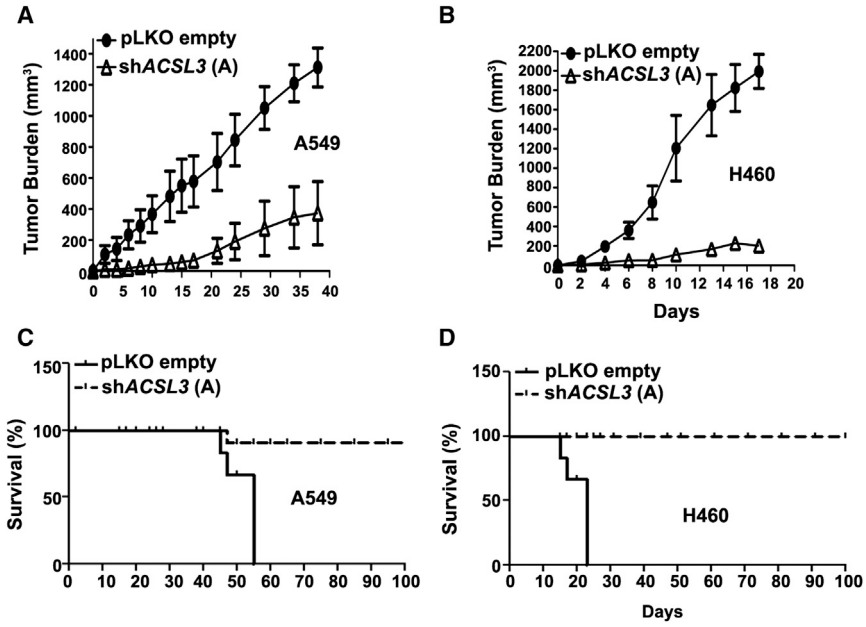

Figure 5. *ACSL3* Suppression Impairs Tumorigenesis In Vivo

(A and B) Tumor volume of xenografts of A549 and H460 NSCLC cells upon transduction with the indicated shRNAs.

(C and D) Kaplan-Meier curves of nude mice carrying xenografts of A549 and H460 NSCLC cells expressing the indicated shRNA upon transduction with lentiviruses (n = 6/group).

(Figure 6F). We used the Aperio Image Toolbox (Leica Biosystems) to quantify ACSL3 staining in lung cancer specimens with a scoring scale, which takes into consideration the staining intensity in conjunction with the percentage of positive cells (H-score; ranging from 0 to 300). We considered an H-score of less than 100, from 100 to 200, and above 201 having a low, intermediate, or high staining intensity, respectively. Overall, there was a higher percentage of samples with the higher H-score of >201 (Figure S5H). However, there was no significant difference between the H-score of wild-type and mutant *KRAS* NSCLC samples (Figure S5I). Notably, a significantly higher percentage of surgical stage I (early stage) specimens displayed a higher H-score as compared to stage III specimens (late stage; Figures 6G and S5J). We conclude that ACSL3 is highly expressed in lung cancer. These results also suggest that ACSL3 may play an important role in the early stages of tumorigenesis, a notion that is consistent with our findings that ACSL3 is required for tumor initiation in the *LSL-Kras*^{G12D} mouse model of lung tumorigenesis (Figures 6A and 6B).

DISCUSSION

The observation that extinction of mutant *Kras* in vivo causes a prominent perturbation of the glycolytic and lipid metabolic pathways in lung cancer cells suggests that these networks are involved in lung cancer maintenance.

Glucose metabolism has been intensely studied in cancer cell lines and tumors. Mutant *KRAS* induces aerobic glycolysis in vitro and in vivo in mouse models of pancreatic and lung cancer (Racker et al., 1985; Ying et al., 2012). Furthermore, abrogation of the glycolytic enzymes *Hk2* and *Ldh-A* impairs without abolishing the formation of mutant *Kras* lung tumors in mice (Patra et al., 2013; Xie et al., 2014). Our finding that suppression of glycolytic enzymes reduces the proliferation of mutant *KRAS* NSCLC cells without causing cell death in cell culture is consistent with these recent reports and suggests that alternative bioenergetic pathways, particularly those that oxidize FAs, glutamine, or other nutrients, may support the survival of mutant *KRAS* lung cancer cells, providing mechanisms that bypass the inhibition of HK2, LHD-A, or other glycolytic enzymes (Boroughs and DeBerardinis, 2015).

We obtained several lines of evidence that *ACSL3* is the critical ACSL enzyme required not only for the viability of mutant *KRAS* NSCLC cells in culture but also for the ability of mutant *Kras* to promote tumor initiation and progression in vivo. The observation that, in human NSCLC specimens, ACSL3 is readily detected adds support to the notion that ACSL3 plays a role in NSCLC tumorigenesis. Longer follow-up will be needed to fully characterize the phenotype of *Acsl3*$^{-/-}$ lung tumors, but taken together, our data demonstrate that *ASCL3* is a critical requirement for mutant *KRAS* lung tumorigenesis.

Cancer cells display the ability to both synthetize FAs de novo and to uptake them from extracellular sources (Boroughs and DeBerardinis, 2015). We reason that the dependency on ACSL3 is due to several properties of this enzyme. ACSL3 is placed at a critical metabolic node because ACSL enzymes are essential for both β-oxidation and lipid biosynthesis by activating long-chain FAs derived from either an exogenous or endogenous source. Our observation that suppression of ACSL3 leads to significant inhibition of β-oxidation with depletion of cellular ATP, loss of mitochondrial function, and impaired cell viability underscores the importance of this enzyme in mutant KRAS lung cancer cells. Furthermore, we demonstrated that mutant KRAS promotes the cellular accumulation of neutral lipids (which are mostly by TAGs) in an *ACSL3*-dependent manner. We speculate that lipid droplets, the organelles that store neutral lipids, may provide substrates that support β-oxidation in conditions of energetic stress, particularly in vivo. Therefore, we conclude that ACSL3 is a critical non-redundant therapeutic target for cancer types that rely on lipid metabolic processes.

From a therapeutic point of view, it is also of interest that even a partial decrease in ACSL enzymatic activity is sufficient to achieve a critical therapeutic threshold without causing generalized toxicity in cultured cells or major phenotypes in *Acsl3*-null mice. These observations suggest that ACSL3 is limiting in

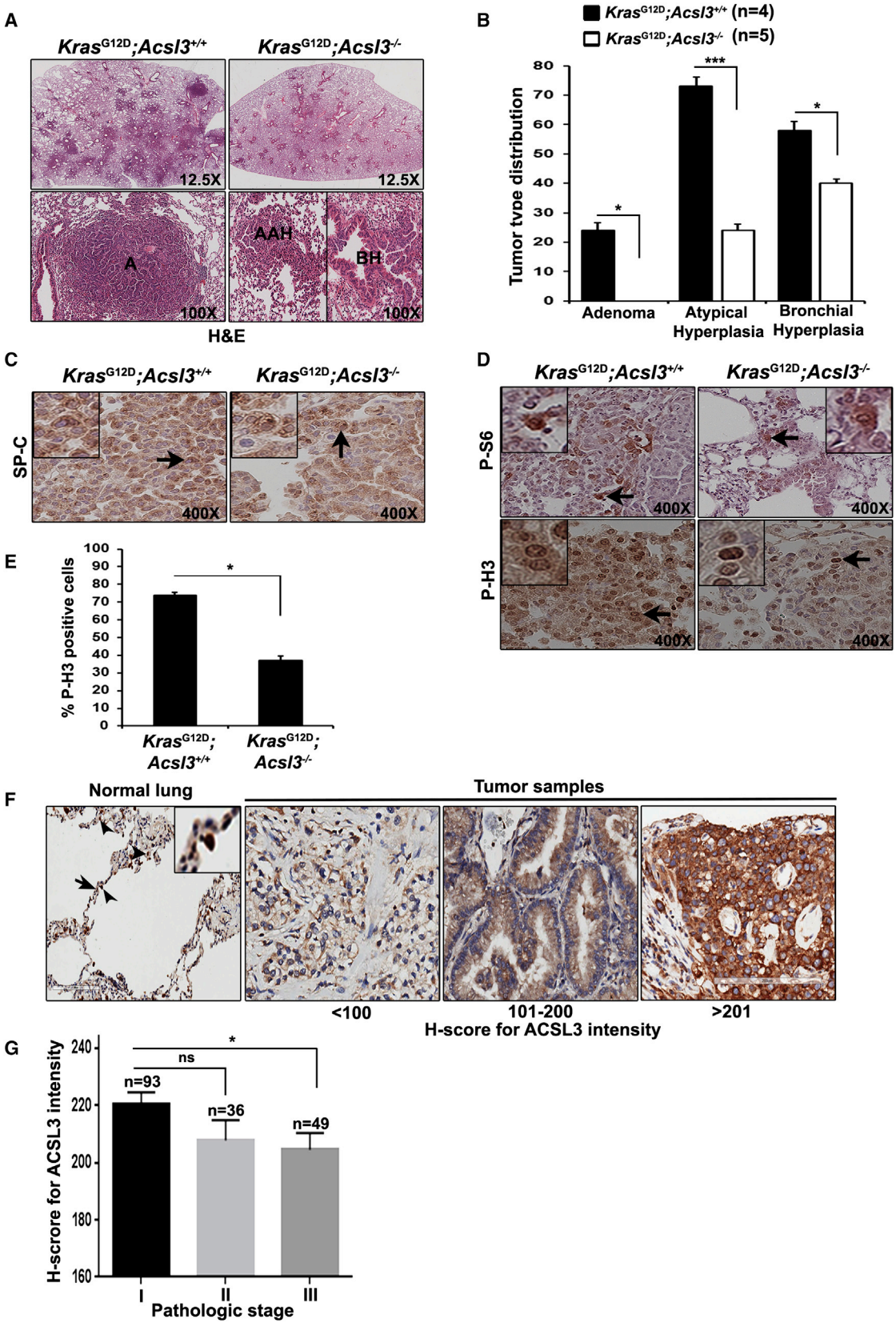

(legend on next page)

conditions of oncogenic stress. Accordingly, inhibition of ACSL3 is likely to have a therapeutic window in vivo.

Moreover, ACSL3 is distal to FASN, where compensatory mechanisms are less likely to occur (Coleman et al., 2002; Menendez and Lupu, 2007). For instance, others have reported that ACSL short-chain family member 2 (ACAS2) and FASN, which are upstream of ACSL in de novo FA synthesis, may represent therapeutic targets (Hatzivassiliou et al., 2005; Menendez and Lupu, 2007). However ACL and ACAS2 may compensate for each other, whereas the requirement for FASN may be bypassed by the uptake of exogenous lipids. In these regards, our findings also provide a molecular explanation to the recent observation that mutant KRAS promotes the scavenging of longer-chain unsaturated FAs from lipids in the extracellular space. In addition, these serum lipids are shown to promote both proliferation and survival of Ras-driven human cancer cells (Kamphorst et al., 2013; Salloum et al., 2014).

Our results suggest that the catalytic activity is required for the vulnerability to ACSL3 depletion in mutant KRAS NSCLC. However, we were unable to rescue the viability defect caused by ACSL3 suppression with short-chain FAs that enter the mitochondrion in a CPT1A-independent manner. We reason that, in addition to defective β-oxidation, several other processes could contribute to the dependency of mutant *KRAS* lung cancer cells on ACSL3. For instance, ACSL enzymes also provide substrates for protein lipidation, such as farnesylation and myristoylation, which are required for the activity of several oncogenes, including KRAS (Gysin et al., 2011). It is also possible that these important long-chain acyl-CoAs cannot be replenished by supplementing medium-chain free FAs. Contrary to our expectation, we did not detect changes in phospholipid content upon ACSL3 silencing; thus, we reason that it is not likely that a defect in the synthesis of cellular membranes causes the loss of viability of NSCLC cells, at least during the time frame of our experiments (Yao and Ye, 2008). In principle, inhibition of ACSL3 could also lead to the accumulation of cytotoxic free FAs; however, our mass spectrometry data do not provide support to this hypothesis. Future studies will be necessary to understand in greater detail the mechanisms responsible for the dependency of mutant *KRAS* lung cancer cells on *ACSL3*.

The results of our transactivation assays are consistent with the notion that mutant KRAS regulates the *ACSL3* promoter through mTORC1, which is a well-known regulator of the SREBPs prolipogenic transcription factors, which in turn may promote aberrant proliferation in cancer cells (Laplante and Sabatini, 2012). Furthermore, SREBPs are required for aberrant proliferation and survival of breast cancer cells (Ricoult et al., 2016). It is noteworthy that the *ACSL3* and *ACSL4*, but not the *ACSL1* and *ACSL6*, promoters contain SREBP-binding sites. Thus, it is likely that mutant *KRAS* regulates the *ACSL3* promoter through the mTORC1/SREBP pathway. It is also of interest that wild-type *KRAS* NSCLC cells bypass the deleterious effects of *ACSL3* knockdown by upregulating other *ACSL3* family members. Thus, it will be of interest in the future to define in greater detail the mechanisms that regulate the expression of ACSL family members.

Whereas we focused on NSCLCs with *KRAS* mutations, it is likely that the detrimental effects on cell viability of *ACSL3* knockdown are not restricted only to mutant *KRAS* lung cancer cells, as demonstrated by the observation that H661, HCC95, and H125 NSCLC cell lines with wild-type *KRAS* are also sensitive to *ACSL3* knockdown. The observation that a significant percentage of lung tumors with high intensity of ACSL3 staining does not carry mutant *KRAS* suggests that other oncogenic mutations may upregulate ACSL3. Therefore, future studies will be needed to determine the spectrum of lung cancer oncogenotypes vulnerable to ACSL3 depletion.

Our report provides the important demonstration that mutant KRAS positively regulates lipid metabolism, establishing a requirement that can be exploited for therapeutic gain. We propose that ACSL3 is a target for the development of targeted therapies against mutant KRAS lung cancer.

EXPERIMENTAL PROCEDURES

All reagents and detailed methods are described in the Supplemental Information.

Cell Lines, Reagents, and Plasmids

Human NSCLC cell lines and immortalized human bronchial epithelial HBEC3KT cells (which ectopically express *Cdk4* and *hTERT*) were from the Hamon Center cell line repository (UT Southwestern Medical Center; Gazdar et al., 2010; Ramirez et al., 2004). All cell lines were DNA fingerprinted for provenance (PowerPlex 1.2 Kit; Promega) and were mycoplasma free (e-Myco Kit; Boca Scientific). Fluorescent BODIPY-FA was from Molecular

Figure 6. *ACSL3* Is Required for the Initiation of *KRAS*-Driven NSCLC in Mice and Is Expressed in Patients

(A) Images of $Kras^{G12D}$ lung cancers stained with H&E after 8 weeks of adeno-Cre infection. Lung nodules are indicated as A: adenoma, AAH: atypical adenomatous hyperplasia, and BH: bronchial hyperplasia (magnification: upper panels 12.5×; bottom panels 100×).

(B) Histogram of tumor type distribution in mice with the indicated genotypes (*$p < 0.05$; ***$p < 0.001$; n, number of mice samples per genotype). Tumor types are indicated.

(C) Images of murine lung tumors stained with SP-C antibody. Positive staining confirms their origin from type II alveolar cells (magnification 400×). Arrows indicate the location of the inlets.

(D) Images of murine lung tumors stained with indicated antibodies. Antibody staining is in brown; nuclear counter staining is in blue (magnification 400×). Arrows indicate the location of inlets.

(E) The histogram shows the percentage of P-H3-positive cells in lung tumors of $Kras^{G12D}$; $Acsl3^{+/+}$ and $Kras^{G12D}$; $Acsl^{-/-}$ mice (100 cells were counted in three separate areas).

(F) Representative microphotographs of ACSL3 in the indicated representative human samples (respective H-score for tumor samples are indicated). Black arrowhead indicates ACSL3 in type II pneumocytes. Arrows indicate the location of inlet (the scale bar represents 200 μm).

(G) Histogram showing H-score for ACSL3 staining intensity in tumor samples according to their pathologic stages (*$p < 0.05$; ns, statistically insignificant; n, number of patient samples).

See also Figure S5.

Probes, pBabePuro and pBabePuro-*KRAS-G12V* were from Addgene, the *ACSL3* cDNA was from Dr. Takahiro Fujino (Department of Bioscience, Ehime University), and pGL3-ACSL3luc was from Dr. Jingwen Liu (Department of Veterans Affairs Palo Alto Health Care System). We performed site-directed mutagenesis using the Quickchange kit (Agilent). See also Supplemental Information for tissue culture and assay conditions.

Mouse Studies

CCSP-rtTA/Tet-op-Kras (FVB/SV129 mixed background) mice were described previously (Fisher et al., 2001). *Acsl3*$^{-/-}$ mice (LEXKO-011; Lexicon Genetics) were obtained from the European Mouse Mutant Archive. We generated *LSL-KRas*^{G12D};*Ascl3*$^{-/-}$ mice with standard breeding techniques. We performed xenograft studies as previously described (Konstantinidou et al., 2013). For additional details, refer to the Supplemental Information.

Expression Profiling

Gene expression profiles were obtained from micro-dissected lung tumors of 19-week-old mice (Tusher et al., 2001). The data have been deposited in NCBI's GEO and are accessible through GEO: GSE40606. See also Supplemental Information.

RNAi

We obtained *ACSL3* and *ACSL4* or non-targeting small interfering RNAs (siRNAs) (siGenome) and pLKO lentiviral vectors encoding shRNAs from Thermo Scientific. siRNAs were transfected with DharmaFECT 4 Transfection Reagent (Thermo Scientific). See also Supplemental Information.

Quantitative Real-Time PCR

We extracted RNA with a RNA extraction kit (QIAGEN) and used Superscript III (Invitrogen) to generate cDNA and SYBR Green PCR master mix (Applied Biosystems) for quantitative real-time PCR (qRT-PCR) analysis. See also Supplemental Information.

Immunoblotting and Antibodies

We performed immunoblots according to standard procedures (Konstantinidou et al., 2009). A list of the antibodies is provided in the Supplemental Information.

Measurement of ACSL Activity and β-Oxidation

We measured ACSL activity in cell lysates by detecting incorporation of radiolabeled palmitate into palmitoyl-CoA as previously described (Zhou et al., 2007). We measured β-oxidation as described previously (Deberardinis et al., 2006). See also Supplemental Information for details.

Flow Cytometry

We performed flow cytometry to detect the phases of the cell-cycle or BODIPY-FA uptake according to standard procedures (Konstantinidou et al., 2009; Nchoutmboube et al., 2013).

Lactate and Glucose Flux Measurements

Cell culture media was analyzed for glucose and lactate concentration using a NOVA Biomedical Bio-Profile Basic 4 Analyzer, as described previously (Yang et al., 2009).

Microscopy

For BODIPY-FA, immunofluorescent microscopy cells were fixed with 4% formaldehyde in PBS for 20 min. We used Image J software to evaluate fluorescence patterns and intensity (Schneider et al., 2012). For quantification, we analyzed at least 100 cells in three independent fields. Cells positive for BODIPY-FA staining both in the cytoplasm and cell membrane were considered positive.

Statistical Analysis

All data presented are the mean ± SEM or SD of experiments repeated three or more times. We determined significance using two-tailed unpaired Student's t test or the one-way ANOVA test.

ACCESSION NUMBERS

The accession number for the KRAS tumor microarray reported in this paper is GEO: GSE40606.

SUPPLEMENTAL INFORMATION

Supplemental Information includes Supplemental Experimental Procedures, five figures, and one table and can be found with this article online at http://dx.doi.org/10.1016/j.celrep.2016.07.009.

AUTHOR CONTRIBUTIONS

M.S.P., G.K., and P.P.S. designed the experimental plan. M.S.P., G.K., N.V., M. Melegari, S.R., C.Y., and M. Mitsche performed experiments. M.S.P., G.K., N.V., M. Mitsche, J.M., R.J.D., and P.P.S. analyzed the data. K.E.H. and J.D.M. contributed NSCLC cell lines. K.B. and J.W.S. analyzed microarray data from mouse lung tumors. J.L. contributed to the ACSL3 antibody. X.T., J.R.-C., N.K., and I.I.W. performed and analyzed the data of immunohistochemistry on patient specimens. M.S.P., G.K., and P.P.S. wrote the paper. All authors read and approved the final manuscript.

ACKNOWLEDGMENTS

We thank Dr. Harold E. Varmus for providing *CCSP-rtTA/Tet-op-Kras* mice and BK cells and Dr. Luc Girard and Dr. Helen Hobbs (University of Texas Southwestern Medical Center) for sharing bioinformatics data and expertise in lipid analysis, respectively. We also thank Dr. Andrea Rabellino and Dr. Edward Motea for assistance with transactivation assays and flow cytometer, respectively. The following financial support is acknowledged: American Cancer Society Scholar Award 13-068-01-TBG, CDMRP LCRP grant LC110229, CPRIT RP140672, NCI 5P50 CA70907-15, UT Southwestern Friends of the Comprehensive Cancer Center, the Gibson Foundation, and Texas 4000 (to P.P.S.); CPRIT RP140110 (to M.S.P.); CPRIT RP101496 (to G.K.); NCI R01 CA157996-01 and Welch Foundation research grant I-1733 (to R.J.D.); Lung Cancer SPORE (P50CA70907; to J.D.M., P.P.S., J.W.S., K.E.H., and I.I.W.); CPRIT RP120732 and RP110709 (to J.D.M. and K.E.H.); NIH K01GM109317 (to M. Mitsche); and 1P30 CA 142543-01, the Harold C. Simmons Comprehensive Cancer Center through NCI Cancer Center support grant and 2P30CA016672, MD Anderson's Institutional Tissue Bank, and NIH National Cancer Institute (to I.I.W.).

Received: December 29, 2015
Revised: May 24, 2016
Accepted: July 1, 2016
Published: July 28, 2016

REFERENCES

Boroughs, L.K., and DeBerardinis, R.J. (2015). Metabolic pathways promoting cancer cell survival and growth. Nat Cell Biol. *17*, 351–359.

Cancer Genome Atlas Research Network (2014). Comprehensive molecular profiling of lung adenocarcinoma. Nature *511*, 543–550.

Cao, A., Li, H., Zhou, Y., Wu, M., and Liu, J. (2010). Long chain acyl-CoA synthetase-3 is a molecular target for peroxisome proliferator-activated receptor delta in HepG2 hepatoma cells. J Biol Chem. *285*, 16664–16674.

Coleman, R.A., Lewin, T.M., Van Horn, C.G., and Gonzalez-Baró, M.R. (2002). Do long-chain acyl-CoA synthetases regulate fatty acid entry into synthetic versus degradative pathways? J. Nutr. *132*, 2123–2126.

Deberardinis, R.J., Lum, J.J., and Thompson, C.B. (2006). Phosphatidylinositol 3-kinase-dependent modulation of carnitine palmitoyltransferase 1A expression regulates lipid metabolism during hematopoietic cell growth. J. Biol. Chem. *281*, 37372–37380.

DuPage, M., Dooley, A.L., and Jacks, T. (2009). Conditional mouse lung cancer models using adenoviral or lentiviral delivery of Cre recombinase. Nat. Protoc. *4*, 1064–1072.

Fahy, E., Subramaniam, S., Murphy, R.C., Nishijima, M., Raetz, C.R., Shimizu, T., Spener, F., van Meer, G., Wakelam, M.J., and Dennis, E.A. (2009). Update of the LIPID MAPS comprehensive classification system for lipids. J. Lipid Res. *50* (*Suppl*), S9–S14.

Fisher, G.H., Wellen, S.L., Klimstra, D., Lenczowski, J.M., Tichelaar, J.W., Lizak, M.J., Whitsett, J.A., Koretsky, A., and Varmus, H.E. (2001). Induction and apoptotic regression of lung adenocarcinomas by regulation of a K-Ras transgene in the presence and absence of tumor suppressor genes. Genes Dev. *15*, 3249–3262.

Furuta, E., Pai, S.K., Zhan, R., Bandyopadhyay, S., Watabe, M., Mo, Y.Y., Hirota, S., Hosobe, S., Tsukada, T., Miura, K., et al. (2008). Fatty acid synthase gene is up-regulated by hypoxia via activation of Akt and sterol regulatory element binding protein-1. Cancer Res. *68*, 1003–1011.

Gazdar, A.F., Girard, L., Lockwood, W.W., Lam, W.L., and Minna, J.D. (2010). Lung cancer cell lines as tools for biomedical discovery and research. J. Natl. Cancer Inst. *102*, 1310–1321.

Grevengoed, T.J., Klett, E.L., and Coleman, R.A. (2014). Acyl-CoA metabolism and partitioning. Annu. Rev. Nutr. *34*, 1–30.

Guo, J.Y., Karsli-Uzunbas, G., Mathew, R., Aisner, S.C., Kamphorst, J.J., Strohecker, A.M., Chen, G., Price, S., Lu, W., Teng, X., et al. (2013). Autophagy suppresses progression of K-ras-induced lung tumors to oncocytomas and maintains lipid homeostasis. Genes Dev. *27*, 1447–1461.

Gysin, S., Salt, M., Young, A., and McCormick, F. (2011). Therapeutic strategies for targeting ras proteins. Genes Cancer *2*, 359–372.

Hanahan, D., and Weinberg, R.A. (2011). Hallmarks of cancer: the next generation. Cell *144*, 646–674.

Hatzivassiliou, G., Zhao, F., Bauer, D.E., Andreadis, C., Shaw, A.N., Dhanak, D., Hingorani, S.R., Tuveson, D.A., and Thompson, C.B. (2005). ATP citrate lyase inhibition can suppress tumor cell growth. Cancer Cell *8*, 311–321.

Hu, Y., Lu, W., Chen, G., Wang, P., Chen, Z., Zhou, Y., Ogasawara, M., Trachootham, D., Feng, L., Pelicano, H., et al. (2012). K-ras(G12V) transformation leads to mitochondrial dysfunction and a metabolic switch from oxidative phosphorylation to glycolysis. Cell Res. *22*, 399–412.

Jackson, E.L., Willis, N., Mercer, K., Bronson, R.T., Crowley, D., Montoya, R., Jacks, T., and Tuveson, D.A. (2001). Analysis of lung tumor initiation and progression using conditional expression of oncogenic K-ras. Genes Dev. *15*, 3243–3248.

Kamp, F., and Hamilton, J.A. (2006). How fatty acids of different chain length enter and leave cells by free diffusion. Prostaglandins Leukot. Essent. Fatty Acids *75*, 149–159.

Kamphorst, J.J., Cross, J.R., Fan, J., de Stanchina, E., Mathew, R., White, E.P., Thompson, C.B., and Rabinowitz, J.D. (2013). Hypoxic and Ras-transformed cells support growth by scavenging unsaturated fatty acids from lysophospholipids. Proc. Natl. Acad. Sci. USA *110*, 8882–8887.

Kasurinen, J. (1992). A novel fluorescent fatty acid, 5-methyl-BDY-3-dodecanoic acid, is a potential probe in lipid transport studies by incorporating selectively to lipid classes of BHK cells. Biochem. Biophys. Res. Commun. *187*, 1594–1601.

Konstantinidou, G., Bey, E.A., Rabellino, A., Schuster, K., Maira, M.S., Gazdar, A.F., Amici, A., Boothman, D.A., and Scaglioni, P.P. (2009). Dual phosphoinositide 3-kinase/mammalian target of rapamycin blockade is an effective radiosensitizing strategy for the treatment of non-small cell lung cancer harboring K-RAS mutations. Cancer Res. *69*, 7644–7652.

Konstantinidou, G., Ramadori, G., Torti, F., Kangasniemi, K., Ramirez, R.E., Cai, Y., Behrens, C., Dellinger, M.T., Brekken, R.A., Wistuba, I.I., et al. (2013). RHOA-FAK is a required signaling axis for the maintenance of KRAS-driven lung adenocarcinomas. Cancer Discov. *3*, 444–457.

Laplante, M., and Sabatini, D.M. (2012). mTOR signaling in growth control and disease. Cell *149*, 274–293.

Mashima, T., Oh-hara, T., Sato, S., Mochizuki, M., Sugimoto, Y., Yamazaki, K., Hamada, J., Tada, M., Moriuchi, T., Ishikawa, Y., et al. (2005). p53-defective tumors with a functional apoptosome-mediated pathway: a new therapeutic target. J. Natl. Cancer Inst. *97*, 765–777.

Menendez, J.A., and Lupu, R. (2007). Fatty acid synthase and the lipogenic phenotype in cancer pathogenesis. Nat. Rev. Cancer *7*, 763–777.

Mitsche, M.A., McDonald, J.G., Hobbs, H.H., and Cohen, J.C. (2015). Flux analysis of cholesterol biosynthesis in vivo reveals multiple tissue and cell-type specific pathways. eLife *4*, e07999.

Nchoutmboube, J.A., Viktorova, E.G., Scott, A.J., Ford, L.A., Pei, Z., Watkins, P.A., Ernst, R.K., and Belov, G.A. (2013). Increased long chain acyl-Coa synthetase activity and fatty acid import is linked to membrane synthesis for development of picornavirus replication organelles. PLoS Pathog. *9*, e1003401.

Pao, W., Klimstra, D.S., Fisher, G.H., and Varmus, H.E. (2003). Use of avian retroviral vectors to introduce transcriptional regulators into mammalian cells for analyses of tumor maintenance. Proc. Natl. Acad. Sci. USA *100*, 8764–8769.

Patra, K.C., Wang, Q., Bhaskar, P.T., Miller, L., Wang, Z., Wheaton, W., Chandel, N., Laakso, M., Muller, W.J., Allen, E.L., et al. (2013). Hexokinase 2 is required for tumor initiation and maintenance and its systemic deletion is therapeutic in mouse models of cancer. Cancer Cell *24*, 213–228.

Pike, L.S., Smift, A.L., Croteau, N.J., Ferrick, D.A., and Wu, M. (2011). Inhibition of fatty acid oxidation by etomoxir impairs NADPH production and increases reactive oxygen species resulting in ATP depletion and cell death in human glioblastoma cells. Biochim. Biophys. Acta *1807*, 726–734.

Pylayeva-Gupta, Y., Grabocka, E., and Bar-Sagi, D. (2011). RAS oncogenes: weaving a tumorigenic web. Nat. Rev. Cancer *11*, 761–774.

Racker, E., Resnick, R.J., and Feldman, R. (1985). Glycolysis and methylaminoisobutyrate uptake in rat-1 cells transfected with ras or myc oncogenes. Proc. Natl. Acad. Sci. USA *82*, 3535–3538.

Ramirez, R.D., Sheridan, S., Girard, L., Sato, M., Kim, Y., Pollack, J., Peyton, M., Zou, Y., Kurie, J.M., Dimaio, J.M., et al. (2004). Immortalization of human bronchial epithelial cells in the absence of viral oncoproteins. Cancer Res. *64*, 9027–9034.

Ricoult, S.J., Yecies, J.L., Ben-Sahra, I., and Manning, B.D. (2016). Oncogenic PI3K and K-Ras stimulate de novo lipid synthesis through mTORC1 and SREBP. Oncogene *35*, 1250–1260.

Salloum, D., Mukhopadhyay, S., Tung, K., Polonetskaya, A., and Foster, D.A. (2014). Mutant ras elevates dependence on serum lipids and creates a synthetic lethality for rapamycin. Mol. Cancer Ther. *13*, 733–741.

Schiller, H., and Bensch, K. (1971). De novo fatty acid synthesis and elongation of fatty acids by subcellular fractions of lung. J. Lipid Res. *12*, 248–255.

Schneider, C.A., Rasband, W.S., and Eliceiri, K.W. (2012). NIH Image to ImageJ: 25 years of image analysis. Nat. Methods *9*, 671–675.

Singh, A., Greninger, P., Rhodes, D., Koopman, L., Violette, S., Bardeesy, N., and Settleman, J. (2009). A gene expression signature associated with "K-Ras addiction" reveals regulators of EMT and tumor cell survival. Cancer Cell *15*, 489–500.

Soupene, E., and Kuypers, F.A. (2008). Mammalian long-chain acyl-CoA synthetases. Exp. Biol. Med. (Maywood) *233*, 507–521.

Spector, A.A. (1967). The importance of free fatty acid in tumor nutrition. Cancer Res. *27*, 1580–1586.

Sutherland, K.D., Song, J.Y., Kwon, M.C., Proost, N., Zevenhoven, J., and Berns, A. (2014). Multiple cells-of-origin of mutant K-Ras-induced mouse lung adenocarcinoma. Proc. Natl. Acad. Sci. USA *111*, 4952–4957.

Tusher, V.G., Tibshirani, R., and Chu, G. (2001). Significance analysis of microarrays applied to the ionizing radiation response. Proc. Natl. Acad. Sci. USA *98*, 5116–5121.

Xie, H., Hanai, J., Ren, J.G., Kats, L., Burgess, K., Bhargava, P., Signoretti, S., Billiard, J., Duffy, K.J., Grant, A., et al. (2014). Targeting lactate dehydrogenase–a inhibits tumorigenesis and tumor progression in mouse models of lung cancer and impacts tumor-initiating cells. Cell Metab. *19*, 795–809.

Xu, X., Rock, J.R., Lu, Y., Futtner, C., Schwab, B., Guinney, J., Hogan, B.L., and Onaitis, M.W. (2012). Evidence for type II cells as cells of origin of K-Ras-induced distal lung adenocarcinoma. Proc. Natl. Acad. Sci. USA *109*, 4910–4915.

Yamashita, Y., Kumabe, T., Cho, Y.Y., Watanabe, M., Kawagishi, J., Yoshimoto, T., Fujino, T., Kang, M.J., and Yamamoto, T.T. (2000). Fatty acid induced glioma cell growth is mediated by the acyl-CoA synthetase 5 gene located on chromosome 10q25.1-q25.2, a region frequently deleted in malignant gliomas. Oncogene *19*, 5919–5925.

Yang, C., Sudderth, J., Dang, T., Bachoo, R.M., McDonald, J.G., and DeBerardinis, R.J. (2009). Glioblastoma cells require glutamate dehydrogenase to survive impairments of glucose metabolism or Akt signaling. Cancer Res. *69*, 7986–7993.

Yao, H., and Ye, J. (2008). Long chain acyl-CoA synthetase 3-mediated phosphatidylcholine synthesis is required for assembly of very low density lipoproteins in human hepatoma Huh7 cells. J. Biol. Chem. *283*, 849–854.

Ying, H., Kimmelman, A.C., Lyssiotis, C.A., Hua, S., Chu, G.C., Fletcher-Sananikone, E., Locasale, J.W., Son, J., Zhang, H., Coloff, J.L., et al. (2012). Oncogenic Kras maintains pancreatic tumors through regulation of anabolic glucose metabolism. Cell *149*, 656–670.

Young, R.M., Ackerman, D., Quinn, Z.L., Mancuso, A., Gruber, M., Liu, L., Giannoukos, D.N., Bobrovnikova-Marjon, E., Diehl, J.A., Keith, B., and Simon, M.C. (2013). Dysregulated mTORC1 renders cells critically dependent on desaturated lipids for survival under tumor-like stress. Genes Dev. *27*, 1115–1131.

Yun, J., Rago, C., Cheong, I., Pagliarini, R., Angenendt, P., Rajagopalan, H., Schmidt, K., Willson, J.K., Markowitz, S., Zhou, S., et al. (2009). Glucose deprivation contributes to the development of KRAS pathway mutations in tumor cells. Science *325*, 1555–1559.

Zhou, Y., Abidi, P., Kim, A., Chen, W., Huang, T.T., Kraemer, F.B., and Liu, J. (2007). Transcriptional activation of hepatic ACSL3 and ACSL5 by oncostatin m reduces hypertriglyceridemia through enhanced beta-oxidation. Arterioscler. Thromb. Vasc. Biol. *27*, 2198–2205.